Molecular Catalysis 553 (2024) 113780

Contents lists available at ScienceDirect

Molecular Catalysis

journal homepage: www.journals.elsevier.com/molecular-catalysis

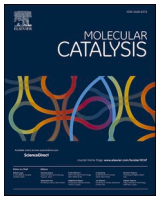

Research Paper

Reaction kinetics of the Shvo-catalyzed dehydrogenation of 1-phenyl-1,3--propanediol-derived lignin model compound

Veronika D Badazhkova [a], Risto Savela [b,c], Johan Wärnå [d], Dmitry Yu Murzin [d], Reko Leino [a,*]

[a] Johan Gadolin Process Chemistry Centre, Laboratory of Molecular Science and Engineering, Organic Chemistry Research Group, Åbo Akademi University, Turku FI-20500, Finland
[b] Turku PET Centre, University of Turku, FI-20520 Turku, Finland
[c] Department of Chemistry, University of Turku, FI-20014 Turku, Finland
[d] Johan Gadolin Process Chemistry Centre, Laboratory of Industrial Chemistry and Reaction Engineering, Åbo Akademi University, Turku FI-20500, Finland

ARTICLE INFO

Keywords:
Shvo-catalyst
Dehydrogenation
Reaction kinetics
Lignin, Biomass

ABSTRACT

The Shvo-catalyst allows to perform hydrogen transfer from the benzylic hydroxyl group of 1-phenyl-1,3-propanediol to 2-butanone. This paper describes kinetic studies on the Shvo-catalyzed dehydrogenation of 1-phenyl-1,3-propanediol as a lignin model compound. The influence of catalyst amount, temperature and the presence of 2-butanol were investigated. It was found that the apparent rate constant of the reaction depends on the catalyst concentration, with the rate expression having 0.5 order in the same. From the study of reaction rates at different temperatures, the apparent activation energy E_a of 1-phenyl-1,3-propanediol conversion was found to be 77 kJ/mol. In the presence of a twenty-fold excess of 2-butanone, the dehydrogenation reaction can be considered as pseudo first order in terms of the substrates. Based on the obtained experimental data, a kinetic model of the dehydrogenation of 1-phenyl-1,3-propanediol, describing the catalyst concentration dependence, temperature influence and the concentrations of 2-butanone and 2-butanol, was developed.

1. Introduction

Lignin, a structural element of lignocellulosic biomass, is a potential sustainable feedstock for manufacturing fuels, fine chemicals, and biomaterials [1]. Structurally, lignin consists of a crosslinked network of aromatic functionalities rich in hydroxyl groups. Further functionalization of the lignin hydroxyl groups serves as a highly useful approach for improving the stability of lignin fractions and imparting desirable properties for synthesis of novel materials and biologically active compounds [2].

New functionalities can be introduced into lignin structures by oxidative dehydrogenation of the hydroxyl groups or, for example, by using hydrogen transfer from a lignin hydroxyl group to an acceptor containing keto group [3]. Previous investigations have proven that hydrogen transfer is a highly selective and safe method, applicable to the hydrogenation of ketones [4–6], aldehydes [7], alkenes [8], alkynes [9] and imines [10,11], dehydrogenation of alcohols [12–14], alkanes [15] and olefins [16], reductive coupling [17], and racemization [18].

For hydrogen transfer reactions, various homogeneous and heterogeneous transition metal catalysts can be utilized [19–28]. Homogeneous ruthenium complexes, in particular, have been frequently employed as catalysts for several organic transformations, including (de)hydrogenations, racemizations and reductive aminations, often displaying high selectivities and product yields [27–31]. Introduced in the early 1980s, the Shvo-catalyst is considered as one of the most active transition metal complexes for hydrogen transfer reactions [32–34]. Dissociation of the Shvo-catalyst into two different complexes allows to perform both dehydrogenation and hydrogenation steps, making it a versatile catalyst applicable for a broad range of hydrogen transfer processes [35,36]. Moreover, the Shvo-catalyzed transfer hydrogenation can be efficiently carried out with low catalyst loadings, under aerobic conditions and mild temperatures (< 100 °C) [37–39].

Originally, the initial dissociation of the Shvo-catalyst has been presumed to form a 16-electron and 18-electron complex, of which the 16-electron [Ru] complex is considered as the active catalyst in dehydrogenation reactions, while the 18-electron hydride complex catalyzes hydrogenation reactions, as illustrated in Scheme 1 [40].

For the dehydrogenation reactions catalyzed by the 16-electron complex, two mechanisms have been proposed: inner and outer sphere, with and without direct bonding of the substrate to the metal

* Corresponding author.
E-mail address: reko.leino@abo.fi (R. Leino).

https://doi.org/10.1016/j.mcat.2023.113780
Received 31 August 2023; Received in revised form 11 December 2023; Accepted 13 December 2023
Available online 18 December 2023

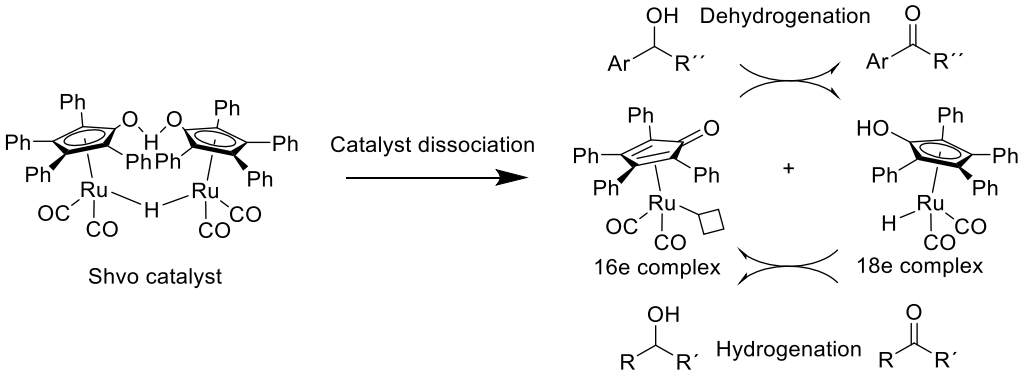

Scheme 1. Catalytic cycle of Shvo-catalyzed hydrogen transfer between the carbonyl and hydroxyl groups, as proposed by Johnson and Bäckvall [40].

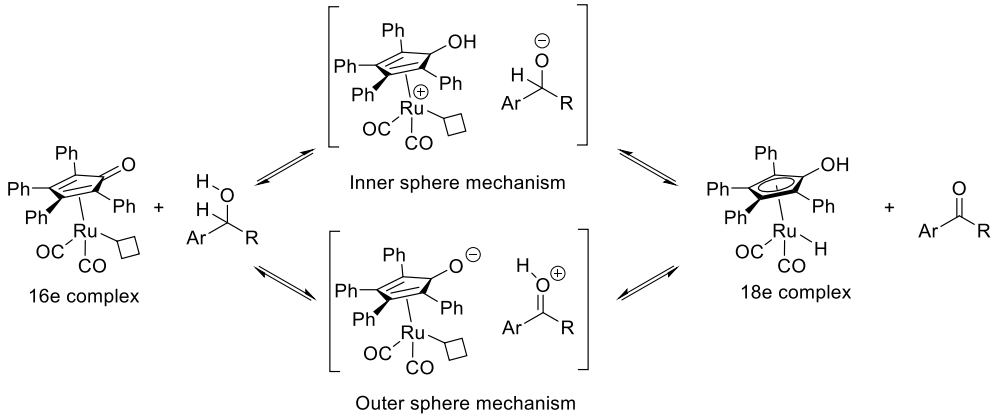

Scheme 2. Alcohol dehydrogenation catalyzed by 16-electron Ru complex via inner and outer sphere mechanism.

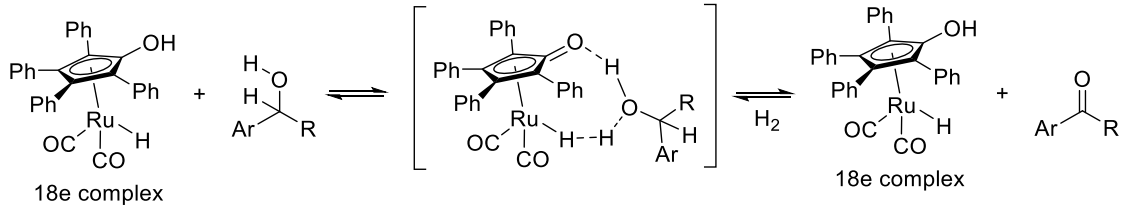

Scheme 3. Alcohol dehydrogenation catalyzed by an 18-electron Ru complex via outer sphere mechanism.

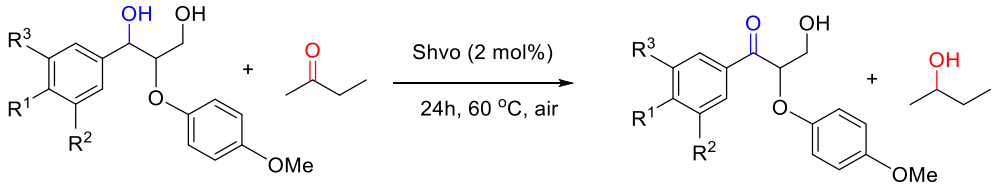

Scheme 4. Shvo-catalyzed dehydrogenation of 1-phenyl-1,2,3-propanetriol derivative, a simple lignin model compound.

center, respectively (Scheme 2) [40].

The formation of a Ru-hydride complex by Shvo catalyst dissociation has been confirmed by ^{1}H and ^{13}C NMR, and IR spectroscopy [41]. The Ru-hydride complex can be easily obtained under hydrogen pressure [41]. However, a 16-elecron complex has never been isolated or directly observed [42,43]. In recent work, Gusev and Spasyuk proposed an alternative mechanism, assuming that dehydrogenation is also catalyzed by an 18 electron Ru complex via outer sphere mechanism (Scheme 3) [43].

In computational studies of Shvo-catalyzed hydrogen transfer, two cases have been proposed and evaluated, both the inner and the outer-sphere mechanisms. In simplified terms, in the former the substrate coordinates directly to the metal center, while in the latter the substrate is interacting via the ligands. The inner sphere mechanism has been largely discredited due to high transition state energy values and, currently, the outer-sphere mechanism without direct coordination to the metal center is considered as the most favorable pathway [44,45].

In recent work, we have developed new methodology for selective

functionalization of the diol fragments in lignin model compounds, using a ruthenium-catalyzed hydrogen borrowing procedure [46]. First, it was demonstrated that the benzylic hydroxyl groups in a simple model compound could be selectively dehydrogenated under aerobic conditions using a homogeneous Shvo-catalyst. Next, this methodology was applied to lignin model compounds containing a diol fragment, and to ethanosolve lignin extracted from milled spruce (Scheme 4). Compared to other recently published protocols [47,48], involving, for example, a metal-free two-step sequence first employing nitrogen monoxide for oxidation followed by hydrazine for reductive C-O bond scission, commercial availability of the Shvo-catalyst, mild conditions of the reaction, and the high yields exceeding 70 %, are the key benefits of our developed approach.

In the present paper, the mechanistic and kinetic details of our earlier synthetic methodology development are addressed in more detail, to facilitate further optimization of the process towards its use for modification of extracted native lignin fractions. Thus, here the reaction kinetics of the Shvo-catalyzed dehydrogenation of 1-phenyl-1,3-propanediol, representing a diol fragment in lignin, using 2-butanone as the hydrogen acceptor, are thoroughly analyzed, and addressed. Several new features of the reaction kinetics, not discussed in previous literature, from the methodological point of view, have been identified and rigorously incorporated into the mathematical modeling. In the present work, reversibility of the reaction was included in the kinetic expression. Here, predominance of noncatalytic dimeric species over the catalytically active monomeric ones results in reaction order below unity. The catalyst has a limited solubility in a particular solvent, resulting in a curve with saturation, which also was considered together with catalyst deactivation. Finally, the significant rate retardation at increasing 2-butanol concentration could be explained by substantially different solubilities of the catalyst in 2-butanone and 2-butanol, respectively, which was treated using the Jouyban-Acree model for solute solubility in binary mixtures of solvents.

2. Experimental

2.1. Material

All chemicals were purchased from TCI, ABCR or Sigma-Aldrich and used without further purification (purity ≥98 %), unless otherwise indicated. Concentrations of the reactants and products were monitored by a gas chromatograph (GC) equipped with flame ionization detector (FID) and an HP-1 column (30 $m \times 320$ μm $\times$ 0.25 μm). Helium was used as the carrier gas with the following temperature program: injector 220 °C, initial oven temperature of 50 °C with 2 min holding time, followed by ramp 10 °C/ min to 300 °C and thereafter hold for 2 min.

2.2. GC/FID calibration

Calibration of GC/FID was performed using diluted solutions of 1-phenyl-1,3-propanediol, 3-hydroxypropiophenone, acetophenone and propiophenone (0.005–0.05 M) containing tetradecane as an internal standard, to obtain the response factors for the main reactants and products. The reference compound was prepared according to a previously published procedure (purity ≥ 95 %) [49].

2.3. General procedure for kinetic measurements at different catalyst loadings

A mixture of solid 1-phenyl-1,3-propanediol 1 (152 mg, 1 mmol), the Shvo catalyst and 2 mL of the tetradecane solution (0.005 M) in 2-butanone were loaded into a two-neck round-bottom flask equipped with a condenser, and heated thereafter to 60 °C. The reaction was monitored for 24 h using GC/FID as described above, withdrawing periodically samples from the reaction mixture. The sets of experiments were carried out at Shvo catalyst loadings of 0.005 mmol (0.5 mol%), 0.01 mmol (1 mol%), 0.02 mmol (2 mol%), 0.03 mmol (3 mol%) and 0.04 mmol (4 mol%).

2.4. General procedure for kinetic measurements at different temperatures

A mixture of solid 1-phenyl-1,3-propanediol (**1**) (152 mg, 1 mmol), the Shvo catalyst (0.02 mmol, 2 mol%) and 2 mL of the tetradecane solution (0.005 M) in 2-butanone were loaded into a two-neck round-bottom flask equipped with a condenser and heated thereafter to the desired reaction temperature. The experiments were carried out at different temperatures of 40 °C, 50 °C, 60 °C, 70 °C and 80 °C.

2.5. General procedure for kinetic measurements of the reactions with 2-butanol addition

A mixture of solid 1-phenyl-1,3-propanediol 1 (152 mg, 1 mmol), the Shvo catalyst (0.02 mmol, 2 mol%), tetradecane solution (0.005 M) in 2-butanone and tetradecane solution (0.005 M) in 2-butanol were loaded into a two-neck round-bottom flask equipped with a condenser and heated thereafter to the desired reaction temperature. The reaction was carried out at different ratios of 2-butanol to 2-butanone to evaluate how the presence of 2-butanol formed in the reaction mixture affects the reaction rate. The total volume of the reaction mixture was equal to 2 mL, thus the concentration of 1-phenyl-1,3-propanediol and tetradecane in the final solution remained constant in each experiment. The reactions were carried out at the 2-butanone:2-butanol ratios of 1 mL:1 mL, 1.5 mL:0.5 mL, 1.9 mL:0.1 mL. The reactions were monitored for 24 h using GC/FID. In all experiments, the overall mass balance was within the experimental errors of GC-FID used to analyze the reaction mixture. However, at higher catalyst concentrations, higher temperatures and longer reaction times, the main product concentration decreased and the peaks of side products including acetophenone and propiophenone started to become visible in GC.

2.6. Kinetic modeling

The rate equations were derived based on the mechanistic models presented below. The parameter estimation was carried out with the software ModEst [50] using as the objective function the squared difference between the experimental and calculated values of the reactant concentrations. This difference was minimized by using the hybrid simplex and Levenberg-Marquardt algorithms. As a descriptor of the quality of the fit, the coefficient of determination R^2, which compares the model performance with respect to the variance of all experimental points, was applied.

For the modeling, all data sets at different temperatures for concentration dependencies with time were used. The rate constants were calculated using the modified Arrhenius equation with the pre-exponential factor corresponding to the rate constant at the average temperature.

$$k = k_0 e^{\frac{-Ea}{R}\left(\frac{1}{T}-\frac{1}{T_{avg}}\right)} \quad (1)$$

Statistical reliability of the constants was evaluated using the Markov Chain Monte Carlo analysis [51], when all the uncertainties in the data and in the modeling were treated as statistical distributions.

3. Results and discussion

3.1. Selection of the model reaction

Based on our previous work, 1-phenyl-1,3-propane diol was here selected as the model compound for kinetic studies of Shvo-catalyzed dehydrogenation of lignin diol model fragments [46]. The use of a model compound instead of native lignin *per se* allows the exclusion of

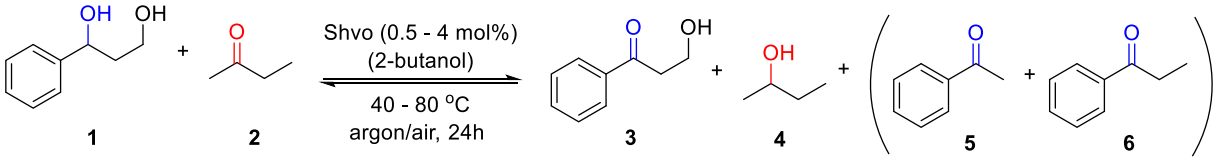

Scheme 5. Shvo-catalyzed dehydrogenation of 1-phenyl-1,3-propanediol with 2-butanone.

Table 1
Rate constants in the dehydrogenation of 1-phenyl-1,3-propanediol (**1**) and the yields of 3-hydroxypropiophenone (**3**) at different catalyst concentrations.

Catalyst amount (mol%)	Apparent rate constant k' (s^{-1})[a,b]	Apparent rate constant k'' (s^{-1} mol%−1)[b,c]	Yield of **3** after 24 h (%)
0.5	1.9×10^{-3}	3.8×10^{-3}	70
1	3.9×10^{-3}	3.9×10^{-3}	80
2	4.7×10^{-3}	2.35×10^{-3}	83
3	5.6×10^{-3}	1.86×10^{-3}	79
4	5.7×10^{-3}	1.35×10^{-3}	77

[a]The rate constant from Eq. (3).
[b]Calculated for the whole concentration domain.
[c]The rate constant from k''=k'/$C_{catalyst}$.

some secondary effects originating from the complexity of the lignin structure, and from the presence of a large number of substituents in the natural material. Moreover, 1-phenyl-1,3-propanediol can be conveniently prepared from commercially available starting material in a facile one-step reaction. The reaction conditions applied in the present investigation were adapted from those developed in our previous work [46]. The reactions were carried out using different catalyst loadings (0.5–4 mol%) and diol (**1**) concentrations (0.25–1 M), also covering the relevant temperature interval of 40–80 °C, as visualized in Scheme 5. The formation of acetophenone (**5**) and propiophenone (**6**) is considered as side degradation reaction of 3-hydroxypropiophenone (**3**). At 60 °C and 2 mol% of catalyst after 24 h, the yields were 3 % for acetophenone (**5**) and 3 % for propiophenone (**6**). Formation of byproducts was considered in the model along with conversion dependent catalyst deactivation. For exploring the influence of the byproduct 2-butanol on the reaction kinetics, different 2-butanone/2-butanol mixtures were investigated as well.

3.2. Formal first order kinetics

The apparent first order rate constants were calculated by fitting each concentration curve to the integral rate expression:

$$C_{1-phenyl-1,3-propanediol} = C^{0}_{1-phenyl-1,3-propanediol} exp(-k't)j \quad (2)$$

The apparent rate constant thus includes the catalyst concentration.

The apparent rate constant of the reaction k', which should be proportional to the catalyst concentration for the first order in the catalyst, in fact increased with the catalyst loading from 0.5 mol% to 3 mol%, but no longer at 4 mol% concentration (Table 1).

The same Table 1 demonstrates a decrease of the apparent rate constant k'', which was presumed to be constant for the first order in the catalyst. A possible explanation for such dependence could be that the reaction order in the catalyst is not equal to unity, as discussed in more detail below.

3.3. Derivation of rate equations

To better understand the influence of the reactants and the reaction conditions on the dehydrogenation outcome, and the uncertainties related to the catalyst loading vs. the stagnating apparent rate of the reaction, kinetic modeling was performed. Based on the plethora of research on the mechanism of transfer hydrogenation reactions [43,52,53], simplified hypothetical outer sphere and inner sphere dehydrogenation catalytic cycles were constructed, as shown in Scheme 4. Here, the starting point was to elucidate and understand the catalytically

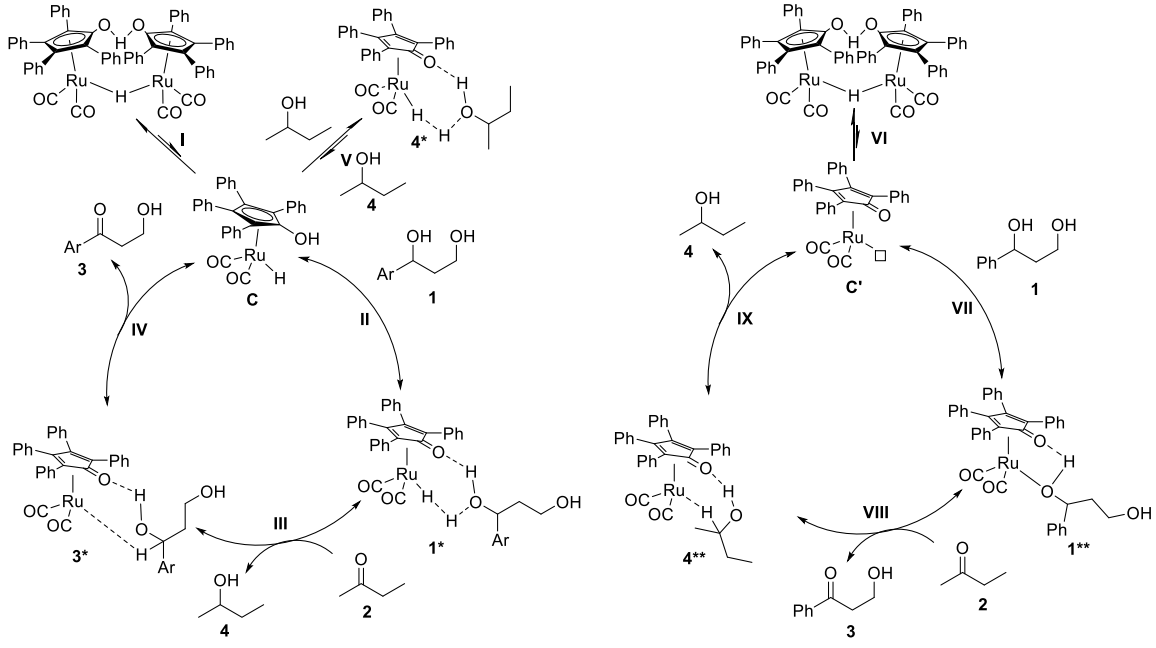

Scheme 6. The outer sphere (left) and inner sphere (right) catalytic cycles for dehydrogenation of 1-phenyl-1,3-propanediol.

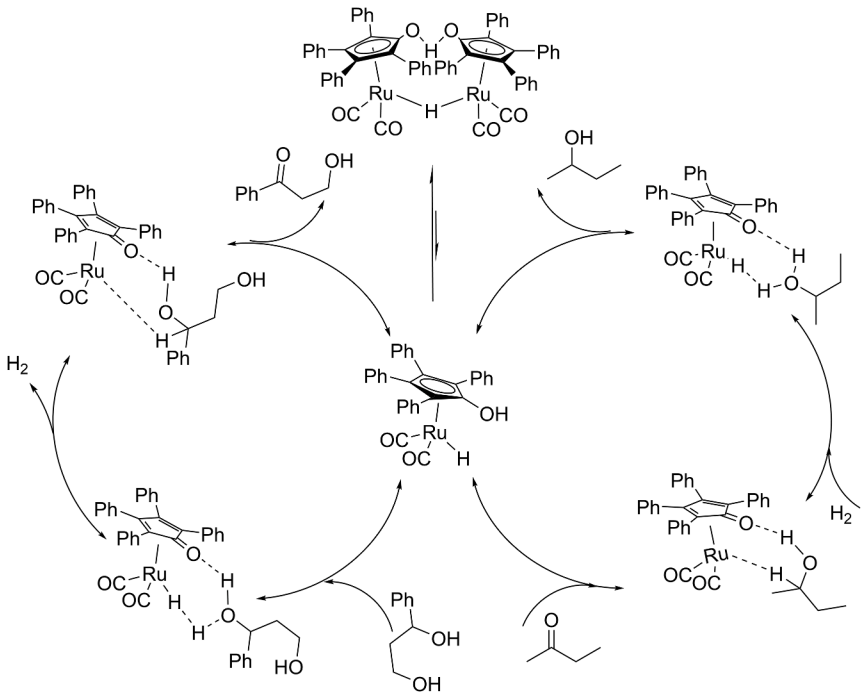

Scheme 7. Outer sphere mechanism of the Shvo-catalyzed dehydrogenation involving two catalytic cycles and a common vertex.

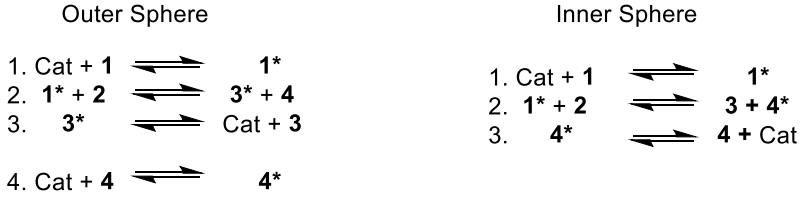

Fig. 1. The elemental steps of outer (left) and inner (right) sphere mechanisms of Shvo-catalyzed dehydrogenation.

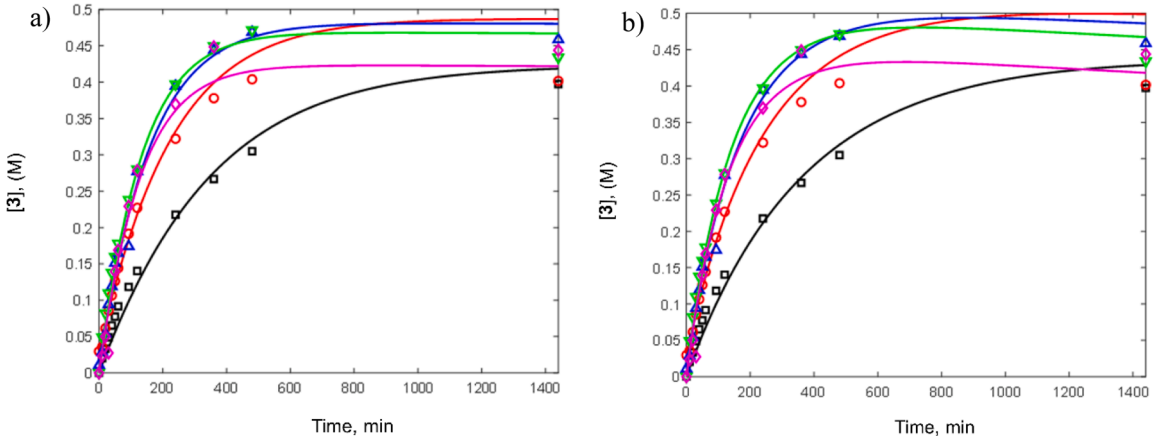

Fig. 2. Concentrations profiles of 3-hydroxypropiophenone formed in the dehydrogenation of 1-phenyl-1,3-propanediol at different catalyst concentrations. The reactions were carried out at 60 °C in 2 mL of 2-butanone with the starting concentration of 1-phenyl-1,3-propanediol equal to 0.5 M with 0.5 mol% (□), 1 mol% (○), 2 mol% (△), 3 mol% (▽) and 4 mol% (◊) of the Shvo-catalyst. Modeling according to (a) Eqs. (12) and (13); and (b) Eqs. (16) and (17).

active species, formed by dissociation of the initial Shvo-catalyst being in equilibrium with the reactive species (Scheme 6, I). Such dissociation is typically considered in a catalytic cycle as a hanging vertex and, consequently, the reaction rate is proportional to the square root of the initial catalyst concentration [52,53], in line with the experimental observations showing deviations from the first order kinetics in the catalyst concentrations. Here, the exact mechanism of the dimeric precursor dissociation to form the active catalyst is not discussed in detail, while used for the purposes of kinetic modeling.

The somewhat simplified version of the outer sphere mechanism without step V (Scheme 6, left side) was initially evaluated. Considering the binding steps II and IV as fast in both directions (i.e., in quasi-

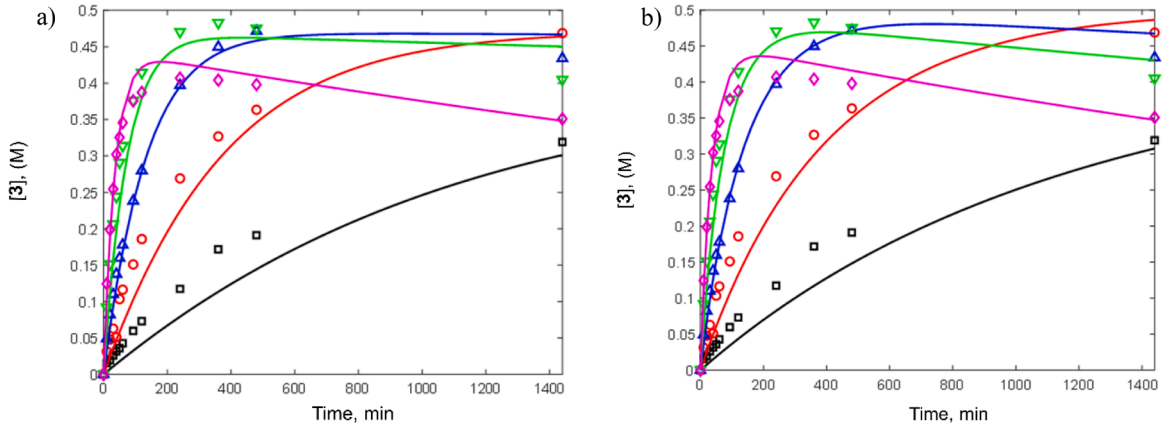

Fig. 3. Concentrations profiles of 3-hydroxypropiophenone formed in the dehydrogenation reaction of 1-phenyl-1,3-propanediol at different temperatures. The experiments were carried out in 2 mL of 2-butanone with the initial concentration of 1-phenyl-1,3-propanediol equal to 0.5 M and 2 mol% of the Shvo-catalyst at 40 °C (□), 50 °C (○), 60 °C (△), 70 °C (▽) and 80 °C (◊). The modeled concentration profiles (*vide infra*) are given as solid lines with colors corresponding to the colors of the experimentally measured data points. Modeling according to a) Eqs. (12) and (13); b) Eqs. (16) and (17).

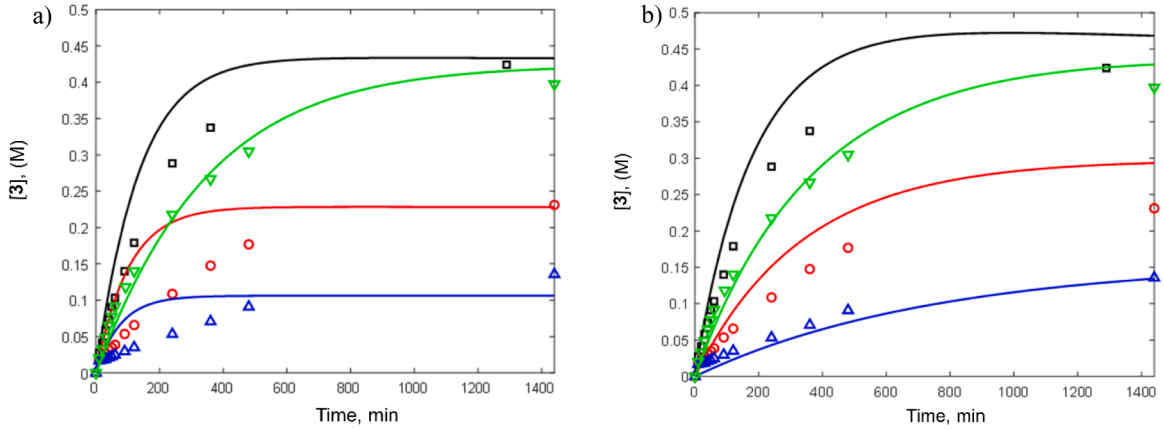

Fig. 4. Concentrations profiles of 3-hydroxypropiophenone at different initial concentrations of 2-butanol. The reactions were carried out at 60 °C with the initial concentration of 1-phenyl-1,3-propanediol equal to 0.5 M and 2 mol% of the Shvo-catalyst in a mixture of 1 mL of 2-butanol and 1 mL of 2-butanone (△), 0.5 mL of 2-butanol and 1.5 mL of 2-butanone (○), 0.1 mL of 2-butanol and 1.9 mL of 2-butanone (▽), 2 mL of 2-butanone (□). The modeled concentration profiles (vide infra) are given as solid lines with colors corresponding to the colors of the experimentally measured data points. Figure a) corresponds to Eqs. (12) and (13); and b) to Eqs. (16) and (17).

Table 2
Values of the kinetic parameters and statistical analysis.

Parameter	Value	Units	Standard error (%)*
$k'_{+2,0}\ K_1\sqrt{y}$	0.378×10^{-3}	L/(mol%)$^{0.5}$ min mol)	7.1
$k'_{-2,0}\ (K_3^{-1})'\ \sqrt{y}$	0.844×10^{-3}	L/(mol%)$^{0.5}$ min mol)	12.7
k_3	$0.42 \times 10^{-}$	1/(mol%)$^{0.5}$/min	42
φ	−7.8	–	7.1
K_s	0.072	(mol%)$^{-1}$	106
$E_{act,1}$	80.9	kJ/mol	3.2
$E_{act,3}$	73.1	kJ/mol	32.4

*The standard error is defined as $SE = \frac{\sigma}{\sqrt{n}}$ with σ=standard deviation, n=number of samples.

equilibria), the corresponding rate expression for this mechanism is:

$$r_{1->3} = \left(k_{+III}K_{II}C_1C_2 - k_{-III}K_{IV}^{-1}C_3C_4\right)\sqrt{C_{cat}} \quad (3)$$

where k_{+III} is the lumped rate constant of step III in the forward direction, also including the catalyst dissociation constant, K_{II} is the equilibrium constant of step II, etc. Based on the preliminary kinetic modeling, a significant decrease in the rate of the reaction with respect to 2-butanol concentration could not be interpreted only through reversibility of the reaction and, consequently, the concentration profiles vs. time dependencies could not be reliably modeled using Eq. (2).

As a first step in improving the kinetic description, binding of 2-butanol to the catalyst was considered in the rate. For the outer sphere mechanism, this should be performed either via out-of-the-cycle quasi-equilibrium step (Scheme 6, V), or as a mechanism involving two routes (Scheme 7) with a common vertex. The latter mechanism implies the release of dihydrogen from the catalyst in one cycle with subsequent involvement of dihydrogen in the other one. In our previous work [46], the release of hydrogen was not detected by ^{1}H NMR, which would either suggest that this mechanism is implausible or that the hydrogen would be present in extremely low quantities and consumed as it is being generated. In the latter case, the corresponding rate constants of dihydrogen release in one cycle and consumption in the other one would be very poorly defined and could not be calculated in a statistically sound way.

For the inner sphere mechanism, the influence of 2-butanol present in the reaction mixture can be considered as a part of the catalytic cycle which, consequently, does not require additional out-of-the-cycle equilibrium for the kinetic modeling. For such variant of the reaction

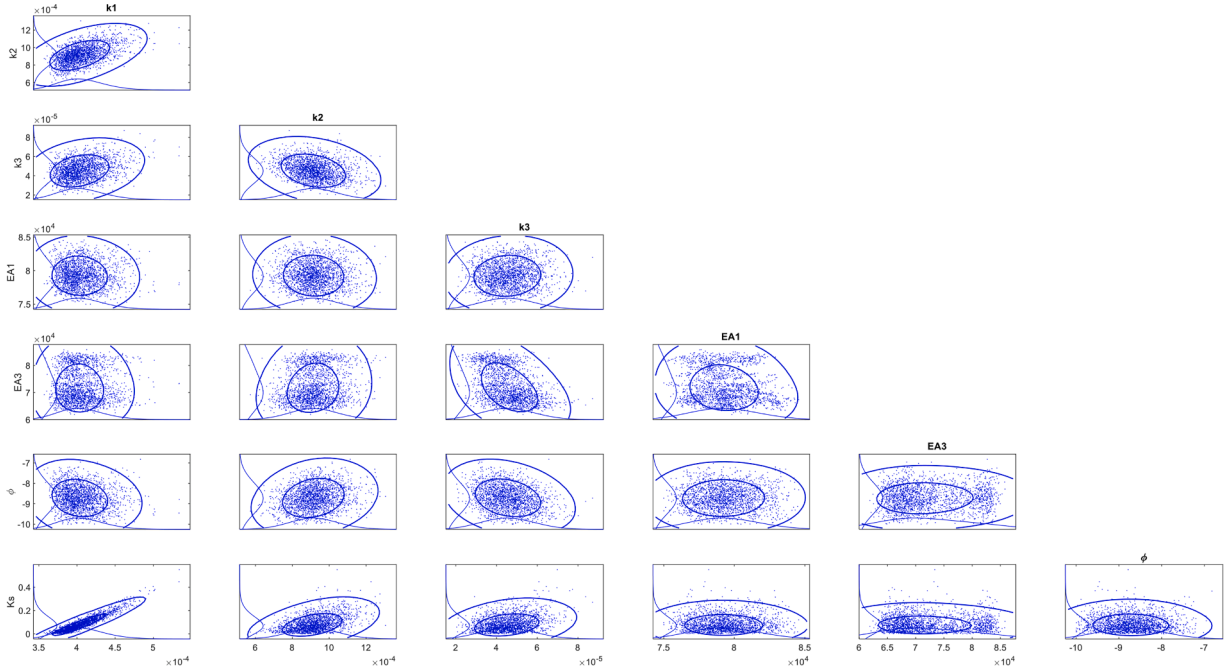

Fig. 5. Contour plots for all parameter combinations.

mechanism, it can be considered that the secondary hydroxyl groups are bound stronger compared to the carbonyl groups. The rate equations for both the outer and inner sphere mechanisms (Scheme 6) can be derived from the elemental steps illustrated in Fig. 1.

Prior to the detailed analysis of such concentration dependencies, a preliminary analysis of the data was performed to evaluate the apparent activation energy.

3.4. Temperature and catalyst concentration dependence

The experimental concentration profiles, obtained from the different catalyst loadings, ranging from 0.5 to 4 mol%, are presented in Fig. 2. Due to the significant excess of 2-butanone, the dehydrogenation reaction can be considered as a pseudo-first order reaction in terms of the substrates [40].

In the series of reactions with different catalyst amounts, it was observed that when the loading exceeds 2 mol% (equal to 10 mg/mL), the catalyst no longer fully dissolves. In previous studies, it has been reported that the solubility of the RuH complex obtained after hydrogenation of Shvo-catalyst varies significantly, depending on the solvent [43]. More detailed data on solubility of the Shvo-catalyst was, however, not accessible in the literature. NMR spectroscopic measurements performed here demonstrated that the Shvo-catalyst has limited solubility, explained by a saturation effect. This conclusion is based on integrals of the aromatic region in the ^{1}H NMR spectra obtained from different catalyst solutions. This dependence was also incorporated in the kinetic modeling. However, due to the presence of Shvo-catalyst in the solution, in the equilibrium between the dimeric and monomeric species, and the high systematic error caused by measurements at low concentrations, it was not possible to calculate the solubility constant of the Shvo-catalyst in 2-butanone.

As follows from Fig. 2, an increase in the catalyst loading after 3 mol % does not increase the rate of the Shvo-catalyzed dehydrogenation reaction. This could be due to, for example, poor catalyst solubility, reversibility of the hydrogen transfer from 1-phenyl-1,3-propanediol to 2-butanone, and/or deactivation of the Shvo-catalyst. All these options were here incorporated in the kinetic expression.

For comparing the activation energy of the Shvo-catalyzed dehydrogenation reaction to previously published data, the effects of temperature on the reaction rate, ranging from 40 °C to 80 °C with 2 mol % of catalyst in 0.5 M solution of 1-phenyl-1,3-propanediol, were investigated. The experimental concentration profiles, obtained at different reaction temperatures are presented in Fig. 3. The apparent activation energy of the Shvo-catalyzed dehydrogenation was evaluated using the Arrhenius equation by plotting lnk' vs 1/T. To compare the obtained value of 77 kJ/mol with the literature data on hydrogen transfer reactions with the Shvo catalyst, activation energies of ~54 kJ/mol for benzaldehyde reduction [44] and ~77 kJ/mol for 1-(4-fluorophenyl)ethanol oxidation [40] can be considered. It can also be noted that the apparent activation energies in related reactions using mononuclear Ru-catalysts have been observed to be in the 83–105 kJ/mol range [54,55] and with cationic Ru-catalysts values as low as 40–60 kJ/mol [56] have been reported for methyl levulinate dehydrogenation.

3.5. The effects of 2-butanol on the reaction rate

Next, the influence of 2-butanol concentration on the rate of the reaction was investigated. Concentration profiles of the reactions were measured using different mixtures of 2-butanol and 2-butanone (Fig. 4). The lumped rate constants determined for the pseudo first order in the substrate concentration were found to be significantly influenced by the 2-butanol concentration (not shown), which further should be considered in mechanistically sound kinetic modeling. The results presented in Fig. 4 clearly show a significant influence of 2-butanol concentration on the apparent rate constant and the yield of the dehydrogenation reaction.

Solubility of the catalyst in 2-butanone/2-butanol was further evaluated by ^{1}H NMR spectroscopy. The NMR spectroscopic measurements demonstrated that shifting of the solvent ratio towards more 2-butanol in the mixture leads to a significant drop in catalyst solubility. However, similar to the solubility experiments in 2-butanone at different catalyst loadings, it was neither possible to calculate the solubility constant of the Shvo-catalyst in 2-butanol mixture.

3.6. Mechanistic kinetic models and numerical data fitting

Based on the preliminary analysis of the data in the Sections 3.2-3.4, it becomes clear that the reaction order in the catalyst is lower than

unity and that reversibility of the reaction should be considered.

For the reaction mechanisms displayed in Fig. 1, the corresponding rate equations can be easily derived, being for the outer sphere mechanism:

$$r_{1->3} = \left(k_{+2}K_1C_1C_2 - k_{-2}K_3^{-1}C_3C_4\right)C_{mono} \quad (4)$$

and for the inner sphere mechanism, respectively:

$$r_{1->3} = \left(k'_{+2}K'_1C_1C_2 - k'_{-2}\left(K_3^{-1}\right)'C_3C_4\right)C_{mono} \quad (5)$$

$$r_{1->3} = \left(k'_{+2,0}K'_1C_1C_2 - k'_{-2,0}\left(K_3^{-1}\right)'C_3C_4\right)\sqrt{\frac{yC_{catalyst}}{1+K_sC_{catalyst}}\exp(-\mathrm{kd}*\mathrm{conversion})}e^{-\frac{E_{act,1}}{R}\left(\frac{1}{T}-\frac{1}{T_{ave}}\right)} \quad (12)$$

Where C_{mono} is the concentration of the monomeric species. As evidently observed, these equations are similar and the modeling was here continued using the inner sphere mechanism-based rate equation (Eq. (5)).

In a general case, both the forward and backward rate constants can have different activation energies. However, the Gibbs energy of the dehydrogenation reactions, due to similarities between the reactants and the products, should be close to zero [57] and, thus, the activation energy for the apparent rate constants in both directions can be considered equal as the first approximation, as illustrated in Eq. (6):

$$r_{1->3} = \left(k'_{+2,0}K'_1C_1C_2 - k'_{-2,0}\left(K_3^{-1}\right)'C_3C_4\right)C_{mono}e^{-\frac{E_{act}}{R}\left(\frac{1}{T}-\frac{1}{T_{ave}}\right)} \quad (6)$$

where T_{ave} is the average T of experiments [58] equal to 60 °C and includes pre-exponential factors for the rate constants. The decrease of 3-hydroxypropiophenone concentration in the reaction mixture is caused by degradation side reaction of 3-hydroxypropiophenone (**3**) to acetophenone (**5**) and propiophenone (**6**). Subsequent transformations of 3-hydroxypropiophenone (**3**) to byproducts were considered by assuming that:

$$r_{3->unknown} = k_3C_3C_{mono} \quad (7)$$

The generation rates of components of the reaction network can be easily written:

$$-\frac{dC_1}{dt} = -\frac{dC_2}{dt} = \frac{dC_4}{dt} = r_{1->3}; \frac{dC_3}{dt} = r_{1->3} - r_{3->unknown}; \frac{dC_{unknown}}{dt} = r_{3->unknown} \quad (8)$$

In separate experiments, it was demonstrated that the catalyst is mainly present in the reaction milieu as a dimer, thus the concentration of the monomer can be simply obtained from the equilibrium of catalyst dimerization. The current case is more complex, as the dimeric form of the catalyst has limited solubility in the liquid displaying a saturation behavior. To address such limited solubility behavior the dissolved concentration of the dimeric form of the catalyst was modeled through the expression, which combines the first order dependence at low concentrations and complete saturation at high catalyst concentrations:

$$C_{dissolved\ dimer} = \frac{yC_{catalyst}}{1+K_sC_{catalyst}} \quad (9)$$

Catalyst deactivation was considered by introducing the activity function, which was dependent on conversion:

$$activity = activity_0 * exp(-k_d * conversion) \quad (10)$$

with the initial activity ($activity_0$) equal to unity. An alternative approach of time dependent deactivation resulted in almost the same degree of explanation.

Considering Eqs. (9) and (10), the concentration of monomers in equilibrium with the dissolved dimer concentration was approximated as:

$$C_{mono} = \sqrt{\frac{yC_{catalyst}}{1+K_sC_{catalyst}}\exp(-k_d*\mathrm{conversion})} \quad (11)$$

Subsequently the rate expressions for the main reaction and side reactions are:

$$r_{3->unknown} = k_3C_3\sqrt{\frac{yC_{catalyst}}{1+K_sC_{catalyst}}\exp(-\mathrm{kd}*\mathrm{conversion})}e^{-\frac{E_{act,3}}{R}\left(\frac{1}{T}-\frac{1}{T_{ave}}\right)} \quad (13)$$

The parameter estimation for the concentration dependencies of the reactants resulted in a reasonably good description of the experimental observations with the coefficient of determination R2 equal to 95.71 %. Results of the calculations (Figs. 2a, 3a) illustrate a good description of the experimental data under different reaction conditions (temperature and catalyst concentrations), which were treated simultaneously. As seen from the modeled concentration profiles, the kinetic model can describe, besides the catalyst concentration dependence, also the influence of the temperature. At the same time the dependence on the concentrations of 2-butanone and 2-butanol (Fig. 4a) cannot be adequately captured, which was attributed to different solubility of the Shvo catalyst in different solvents.

To confirm such hypothesis, separate measurements of the dissolved concentrations of the catalyst were performed indicating a significantly lower solubility of the catalyst in 2-butanol compared to 2-butanone. The log-linear model of Yalkowsky [59] proposed for poorly soluble pharmaceuticals in binary mixtures of solvents gives a possibility to calculate the mole fraction solubility of the solute x_{sol} (or Shvo catalyst in the current case x_{cat}) as a function of the mole fraction solubility in mono solvents $x_{cat\ in\ butanol}$ and $x_{cat\ in\ butanone}$ and the mole fraction of 2-butanol in the binary mixture with 2-butanone:

$$lnx_{cat} = (lnx_{cat\ in\ butanone}) + [ln(x_{cat\ in\ butanol}/x_{cat\ in\ butanone})]\ x_{butanol} \quad (14)$$

Subsequently, Eqs. (12) and (13) are modified to include the parameter λ, which accounts for different solubility as a function of the mole fraction of 2-butanol in the mixture of two solvents

$$l = exp((x_{cat\ in\ butanol}/x_{cat\ in\ butanone})\ x_{butanol}) = \exp(x_{butanol}) \quad (15)$$

with $\varphi = \ln(x_{cat\ in\ butanol}/x_{cat\ in\ butanone})$.

While Eq. (15) has a form, which can be easily implemented for practical purposes, especially for a limited set of experimental data, it is based on the algebraic mixing rule assuming ideal, non-interacting behavior of solvents with the ratio of solvents, surrounding the solute, being the same as in the bulk. More complicated analysis of the solubility of the Shvo catalyst in binary solvent mixtures requires elucidation of the contribution of two-body (solute-solvent 1, solute-solvent 2, solvent 1 – solvent 2) and three-body interactions (solute-solvent 1-solvent 2) [59] and is clearly beyond the scope of this work.

The final kinetic expressions for this model are:

$$r_{1->3} = \left(k'_{+2,0}K'_1C_1C_2 - k'_{-2,0}\left(K_3^{-1}\right)'C_3C_4\right)\sqrt{\frac{y\lambda C_{catalyst}}{1+K_sC_{catalyst}}\exp(-k_d*\text{conversion})}e^{-\frac{E_{act,1}}{R}\left(\frac{1}{T}-\frac{1}{T_{ave}}\right)} \quad (16)$$

$$r_{3->unknown} = k_3C_3\sqrt{\frac{y\lambda C_{catalyst}}{1+K_sC_{catalyst}}\exp(-k_d*\text{conversion})}e^{-\frac{E_{act,3}}{R}\left(\frac{1}{T}-\frac{1}{T_{ave}}\right)} \quad (17)$$

While coefficient of determination R2 is almost the same for the modified model, being 96.52 %, and the description of the catalyst concentration and temperature dependencies are similar to the previous model (Figs. 2 and 3), there is apparently a much better description of the influence of 2-butanone and 2-butanol concentrations (Fig. 4). During parameter estimation, the value of the deactivation constant could not be reliably identified. Subsequently, the Markov Chain Monte Carlo analysis [49] was performed to determine this parameter. Such analysis indicated a clear maximum of this value, which was then fixed to k_d=0.08.

The values of other kinetic parameters are shown in Table 2, exhibiting low standard errors for all parameters, apart from K_s.

From the Markov Chain Monte Carlo analysis [49] and Fig. 5, displaying contour plots for all parameter combinations, there are practically no correlations between parameters which would be visible from an elongated shape. The value of parameter φ is negative, reflecting significantly poorer solubility of the catalyst in 2-butanol, compared to 2-butanone.

4. Conclusions

Despite the broad range of application of Shvo-catalyst for hydrogen transfer reactions, detailed kinetic studies on alcohol dehydrogenation reactions, except theoretical computational studies, have not been reported previously. In the present work, we have carried out detailed kinetic studies on the Shvo-catalyzed dehydrogenation of 1-phenyl-1,3-propanediol with 2-butanone as the dihydrogen acceptor, revealing reaction kinetic regularities. The reaction order in the catalyst was below unity, in line with the proposed reaction mechanism, presuming dissociation of the initial catalyst structure into two complexes. A strong dependence in the byproduct concentration was established, resulting in the development of a kinetic model capable of accurately describing the concentration profiles of the reactants and products.

CRediT authorship contribution statement

Veronika D Badazhkova: Investigation, Conceptualization, Writing – original draft, Writing – review & editing. **Risto Savela:** Conceptualization, Writing – review & editing, Supervision. **Johan Wärnå:** Formal analysis, Conceptualization, Writing – review & editing. **Dmitry Yu Murzin:** Formal analysis, Conceptualization, Writing – review & editing. **Reko Leino:** Conceptualization, Writing – review & editing, Supervision.

Declaration of Competing Interest

The authors declare that they have no known competing financial interests or personal relationships that could have appeared to influence the work reported in this paper.

Data availability

Data will be made available on request.

Acknowledgment

Reko Leino and Veronika D. Badazhkova thank the Finnish Natural Resources Research Foundation (grant #20210053) and Åbo Akademi University for financial support.

Supplementary materials

Supplementary material associated with this article can be found, in the online version, at doi:10.1016/j.mcat.2023.113780.

References

[1] C. Li, X. Zhao, A. Wang, G.W. Huber, T. Zhang, Catalytic transformation of lignin for the production of chemicals and fuels, Chem. Rev. 115 (2015) 11559–11624, https://doi.org/10.1021/acs.chemrev.5b00155.
[2] S. Laurichesse, L. Avérous, Chemical modification of lignins: towards biobased polymers, Prog. Polym. Sci. 39 (2014) 1266–1290, https://doi.org/10.1016/j.progpolymsci.2013.11.004.
[3] Z. Zhang, C.W. Lahive, D.S. Zijlstra, Z. Wang, P.J. Deuss, Mild organosolv lignin extraction with alcohols: the importance of benzylic alkoxylation, ACS Sustain. Chem. Eng. 7 (2019) 12105–12116, https://doi.org/10.1021/acssuschemeng.9b07222.
[4] T. Ikariya, A. Blacker, Asymmetric transfer hydrogenation of ketones with bifunctional transition metal-based molecular catalysts, Acc. Chem. Res. 40 (2007) 1300–1308, https://doi.org/10.1021/ar700134q.
[5] S. Hashiguchi, A. Fujii, J. Takehara, T. Ikariya, R. Noyori, Asymmetric transfer hydrogenation of aromatic ketones catalyzed by chiral ruthenium(II) complexes, J. Am. Chem. Soc. 117 (1995) 7562–7563, https://doi.org/10.1021/ja00133a037.
[6] A. Fujii, S. Hashiguchi, N. Uematsu, T. Ikariya, R. Noyori, Ruthenium(II)-catalyzed asymmetric transfer hydrogenation of ketones using a formic acid-triethylamine mixture, J. Am. Chem. Soc. 118 (1996) 2521–2522, https://doi.org/10.1021/ja954126l.
[7] R. Ghosh, N. Jana, S. Panda, B. Bagh, Transfer hydrogenation of aldehydes and ketones in air with methanol and ethanol by an air-stable ruthenium–triazole complex, ACS Sus. Chem. Eng. 9 (2021) 4903–4914, https://doi.org/10.1021/acssuschemeng.1c00633.
[8] S. Horn, M. Albrecht, Transfer hydrogenation of unfunctionalised alkenes using n-heterocyclic carbeneruthenium catalyst precursors, Chem. Commun. 47 (2011) 8802–8804, https://doi.org/10.1039/c1cc12923f.
[9] S. Fu, N. Chen, X. Liu, Z. Shao, S. Luo, Q. Liu, Ligand-controlled cobalt-catalyzed transfer hydrogenation of alkynes: stereodivergent synthesis of Z- and E-alkenes, J. Am. Chem. Soc. 138 (2016) 8588–8594, https://doi.org/10.1021/jacs.6b04271.
[10] N. Uematsu, A. Fujii, S. Hashiguchi, T. Ikariya, R. Noyori, Asymmetric transfer hydrogenation of imines, J. Am. Chem. Soc. 118 (1996) 4916–4917, https://doi.org/10.1021/ja960364k.
[11] J.S.M. Samec, J.E. Bäckvall, Ruthenium-catalyzed transfer hydrogenation of imines by propan-2-ol in benzene, Chem. Eur. J. 8 (2002) 2955–2961, https://doi.org/10.1002/1521-3765(20020703)8:13≤2955::AID-CHEM2955≥3.0.CO;2-Q.
[12] M. Bertoli, A. Choualeb, A. Lough, B. Moore, D. Spasyuk, D. Gusev, Osmium and ruthenium catalysts for dehydrogenation of alcohols, Organometallics 30 (2011) 3479–3482, https://doi.org/10.1021/om200437n.
[13] A. Royer, T. Rauchfuss, D. Gray, Organoiridium pyridonates and their role in the dehydrogenation of alcohols, Organometallics 29 (2010) 6763–6768, https://doi.org/10.1021/om100901b.
[14] B. Stoltz, Palladium catalyzed aerobic dehydrogenation: from alcohols to indoles and asymmetric catalysis, Chem. Lett. 33 (2004) 362–367, https://doi.org/10.1246/cl.2004.362.
[15] I. Göttker-Schnetmann, P. White, M. Brookhart, Iridium bis(phosphinite) p-XPCP pincer complexes: highly active catalysts for the transfer dehydrogenation of alkanes, J. Am. Chem. Soc. 126 (2004) 1804–1811, https://doi.org/10.1021/ja0385235.
[16] G. Zhang, Z. Yin, J. Tan, Cobalt(II)-catalysed transfer hydrogenation of olefins, RSC Adv. 6 (2016) 22419–22423, https://doi.org/10.1039/c6ra02021f.
[17] C. Santana, M. Krische, From hydrogenation to transfer hydrogenation to hydrogen auto-transfer in enantioselective metal-catalyzed carbonyl reductive coupling:

past, present, and future, ACS Catal. 11 (2021) 5572–5585, https://doi.org/10.1021/acscatal.1c01109.
[18] T. Jerphagnon, R. Haak, F. Berthiol, A.J.A. Gayet, V. Ritleng, A. Holuigue, N. Pannetier, M. Pfeffer, A. Voelkin, L. Lefort, G. Verzijl, C. Tarabiono, D. B. Janssen, A.J. Minnaard, B.L. Feringa, J.G. de Vries, Ruthenacycles and iridacycles as catalysts for asymmetric transfer hydrogenation and racemisation, Top. Catal. 53 (2010) 1002–1008, https://doi.org/10.1007/s11244-010-9569-6.
[19] S. Arita, T. Koike, Y. Kayaki, T. Ikariya, Aerobic oxidation of alcohols with bifunctional transition-metal catalysts Bearing C–N chelate ligands, Chem. Asian J. 3 (2008) 1479–1485, https://doi.org/10.1002/asia.200800137.
[20] R. Malacea, R. Poli, E. Manoury, Asymmetric hydrosilylation, transfer hydrogenation and hydrogenation of ketones catalyzed by iridium complexes, Coord. Chem. Rev. 254 (2010) 729–752, https://doi.org/10.1016/j.ccr.2009.09.033.
[21] X. Yu, S. Wan, W. Zhou, 1,4-Reduction of α,β-unsaturated ketones through rhodium (III)-catalyzed transfer hydrogenation, Synlett 33 (2022) 1399–1402, https://doi.org/10.1055/s-0042-1752986.
[22] R.M. Betancourt, P. Phansavath, V. Ratovelomanana-Vidal, Rhodium-catalyzed asymmetric transfer hydrogenation/dynamic kinetic resolution of 3-benzylidene-chromanones, Org. Lett. 23 (2021) 1621–1625, https://doi.org/10.1021/acs.orglett.1c00047.
[23] D. Zakgeym, T. Engl, Y. Mahayni, K. Müller, M. Wolf, P. Wasserscheid, Development of an efficient Pt/Sio2 catalyst for the transfer hydrogenation from perhydro-dibenzyltoluene to acetone, Appl. Catal. A Gen. 639 (2022), 118644, https://doi.org/10.1016/j.apcata.2022.118644.
[24] X. Wu, C. Wang, J. Xiao, Asymmetric transfer hydrogenation in water with platinum group metal catalysts, Platinum Met. Rev. 54 (2010) 3–19, https://doi.org/10.1595/147106709X481372.
[25] J. Ito, H. Nishiyama, Recent topics of transfer hydrogenation, Tetrahedron Lett. 55 (2014) 3133–3146, https://doi.org/10.1016/j.tetlet.2014.03.140.
[26] D. Zhang, F. Ye, T. Xue, Y. Guan, Y. Wang, Transfer hydrogenation of phenol on supported pd catalysts using formic acid as an alternative hydrogen source, Catal. Today 234 (2014) 133–138, https://doi.org/10.1016/j.cattod.2014.02.039.
[27] F. Zaccheria, N. Ravasio, R. Psaro, A. Fusi, Synthetic scope of alcohol transfer dehydrogenation catalyzed by Cu/Al2O3: a new metallic catalyst with unusual selectivity, Chem. Eur. J. 12 (2006) 6426–6431, https://doi.org/10.1002/chem.200501619.
[28] D. Wang, D. Astruc, The golden age of transfer hydrogenation, Chem. Rev. 115 (2015) 6621–6686, https://doi.org/10.1021/acs.chemrev.5b00203.
[29] B. Štefane, F. Požgan, G. Guillena, D. Ramón, Metal-catalysed transfer hydrogenation of ketones. Hydrogen Transfer Reactions. Topics in Current Chemistry Collections, Springer, Cham, 2016, pp. 1–67, https://doi.org/10.1007/978-3-319-43051-5_1.
[30] M. Sun, S. Ge, J. Zhao, R. McDonald, G. Ma, Ruthenium(II) phosphine/picolylamine dichloride complexes hydrogenation and DFT calculations, Catalysts 12 (2022) 377, https://doi.org/10.3390/catal12040377.
[31] S. Enthaler, B. Hagemann, S. Bhor, G. Anilkumar, M. Tse, B. Bitterlich, K. Junge, G. Erre, M. Beller, New ruthenium catalysts for asymmetric transfer hydrogenation of prochiral ketones, Adv. Synth. Catal. 349 (2007) 853–860, https://doi.org/10.1002/adsc.200600475.
[32] M.C. Warner, C.P. Casey, J.E. Bäckvall, T. Ikariya, M. Shibasaki, Shvo's catalyst in hydrogen transfer reactions, in: Bifunctional Molecular Catalysis, 37, Springer, Berlin, Heidelberg, 2011, pp. 85–125, https://doi.org/10.1007/3418_2011_7. Topics in Organometallic Chemistry,.
[33] X. Dou, T. Hayashi, Synthesis of planar chiral shvo catalysts for asymmetric transfer hydrogenation, Adv. Synth. Catal. 358 (2016) 1054–1058, https://doi.org/10.1002/adsc.201501162.
[34] B. Conley, M. Pennington-Boggio, E. Boz, T.J. Williams, Discovery, applications, and catalytic mechanisms of Shvo's catalyst, Chem. Rev. 110 (2010) 2294–2312, https://doi.org/10.1021/cr9003133.
[35] Y. Shvo, D. Czarkie, Y. Rahamim, D.F. Chodosh, A new group of ruthenium complexes: structure and catalysis, J. Am. Chem. Soc. 108 (1986) 7400–7402, https://doi.org/10.1021/ja00283a041.
[36] J.H. Choi, N. Kim, Y.J. Shin, J.H. Park, J. Park, Heterogeneous Shvo-type ruthenium catalyst: dehydrogenation of alcohols without hydrogen acceptors, Tetrahedron lett 45 (2004) 4607–4610, https://doi.org/10.1016/j.tetlet.2004.04.113.
[37] E.V. Johnston, E.A. Karlsson, L.H. Tran, B. Åkermark, J.E. Bäckvall, Efficient aerobic ruthenium-catalyzed oxidation of secondary alcohols by the use of a hybrid electron transfer catalyst, Eur. J. Org. Chem. (2010) 1971–1976, https://doi.org/10.1002/ejoc.201000033.
[38] B.P. Babu, Y. Endo, J.E. Bäckvall, Biomimetic aerobic oxidation of amino alcohols to lactams, Chem. Eur. J. 18 (2012) 11524–11527, https://doi.org/10.1002/chem.201202080.
[39] Y. Endo, J.E. Bäckvall, Aerobic lactonization of diols by biomimetic oxidation, Chem. Eur. J. 17 (2011) 12596–12601, https://doi.org/10.1002/chem.201102168.
[40] J.B. Johnson, J.E. Bäckvall, Mechanism of ruthenium-catalyzed hydrogen transfer reactions. concerted transfer of OH and CH hydrogens from an alcohol to a (cyclopentadienone)ruthenium complex, J. Org. Chem. 68 (2003) 7681–7684, https://doi.org/10.1021/jo034634a.
[41] C.P. Casey, S.E. Beetner, J.B. Johnson, Spectroscopic determination of hydrogenation rates and intermediates during carbonyl hydrogenation catalyzed by Shvo's hydroxycyclopentadienyl diruthenium hydride agrees with kinetic modeling based on independently measured rates of elementary reactions, J. Am. Chem. Soc. 130 (2008) 2285–2295, https://doi.org/10.1021/ja077525c.
[42] B.G. Vaz, C.D. Milagre, M.N. Eberlin, H.M. Milagre, Shvo's catalyst in chemoenzymatic dynamic kinetic resolution of amines–inner or outer sphere mechanism? Org. Biomol. Chem. 11 (2013) 6695–6698, https://doi.org/10.1039/C3OB41318G.
[43] D.G. Gusev, D.M. Spasyuk, Revised mechanisms for aldehyde disproportionation and the related reactions of the Shvo catalyst, ACS Catal. 8 (2018) 6851–6861, https://doi.org/10.1021/acscatal.8b01153.
[44] C.P. Casey, S.W. Singer, D.R. Powell, R.K. Hayashi, M. Kavana, Hydrogen transfer to carbonyls and imines from a hydroxycyclopentadienyl ruthenium hydride: evidence for concerted hydride and proton transfer, J. Am. Chem. Soc. 123 (2001) 1090–1100, https://doi.org/10.1021/ja002177z.
[45] A. Comas-Vives, G. Ujaque, A. Lledós, Hydrogen transfer to ketones catalyzed by Shvo's ruthenium hydride complex: a mechanistic insight, Organometallics 26 (2007) 4135–4144, https://doi.org/10.1021/om7004832.
[46] V.D. Badazhkova, R. Savela, R. Leino, Selective modification of hydroxyl groups in lignin model compounds by ruthenium-catalyzed transfer hydrogenation, Dalton Trans. 51 (2022) 6587–6596, https://doi.org/10.1039/D2DT00267A.
[47] L.E. Hofmann, D. Hofmann, L. Prusko, L.M. Altmann, M.R. Heinrich, Sequential cleavage of lignin systems by nitrogen monoxide and hydrazine, Adv. Synth. Catal. 362 (2020) 1485–1489, https://doi.org/10.1002/adsc.201901641.
[48] M. Wang, J. Lu, X. Zhang, L. Li, H. Li, N. Luo, F. Wang, Two-step, catalytic C–C bond oxidative cleavage process converts lignin models and extracts to aromatic acids, ACS Catal. 6 (2016) 6086–6090, https://doi.org/10.1021/acscatal.6b02049.
[49] J. Kim, K. De Castro, M. Lim, H. Rhee, Reduction of aromatic and aliphatic keto esters using sodium borohydride/MeOH at room temperature: a thorough investigation, Tetrahedron 66 (2010) 3995–4001, https://doi.org/10.1016/j.tet.2010.04.062.
[50] H. Haario, Modelling and Optimization Software ModEst, ProfMath Oy, Helsinki, 2011.
[51] D. Yu. Murzin, J. Wärnå, H. Haario, T. Salmi, Parameter estimation in kinetic models of complex heterogeneous catalytic reactions using bayesian statistics, React. Kinet. Mech. Catal. 133 (2021) 1–15, https://doi.org/10.1007/s11144-021-01974-1.
[52] T. Rosner, J.Le Bars, A. Pfaltz, D.G. Blackmond, Kinetic studies of heck coupling reactions using palladacycle catalysts: experimental and kinetic modeling of the role of dimer species, J. Amer. Chem. Soc. 123 (1998) 1848–1855, https://doi.org/10.1021/ja003191e.
[53] O.N. Temkin, Homogeneous Catalysis with Metal Complexes: Kinetic Aspects and Mechanisms, Wiley, Weinheim, 2012.
[54] Y. Sasson, J. Blum, Dichlorotris(Triphenylphosphine)ruthenium-catalyzed hydrogen transfer from alcohols to saturated and .alpha.,.beta.-unsaturated ketones, J. Org. Chem. 40 (1975) 1887–1896, https://doi.org/10.1021/jo00901a004.
[55] Z.S. Liu, G.L. Rempel, The triphasic transfer hydrogenation of aromatic aldehydes by aqueous sodium formate in the presence of heterogenized ruthenium(II) complexes bound to swellable polymer matrices, J. Mol Cat. A. Chem. 278 (2007) 228–236, https://doi.org/10.1016/j.molcata.2007.09.019.
[56] Q. Peng, X. Zhao, M. Chen, J. Wang, K. Cui, X. Wei, Z. Hou, Cationic Ru complexes anchored on POM via non-covalent interaction towards efficient transfer hydrogenation catalysis, Mol. Catal. 517 (2022), 112049, https://doi.org/10.1016/j.mcat.2021.112049.
[57] D. Geburtig, P. Preuster, A. Bösmann, K. Mueller, P. Wasserscheid, Chemical utilization of hydrogen from fluctuating energy sources – catalytic transfer hydrogenation from charged liquid organic hydrogen carrier systems, Int. J. Hydr. Energy 41 (2016) 1010–1017, https://doi.org/10.1016/j.ijhydene.2015.10.013.
[58] D Yu Murzin, T. Salmi, Catalytic Kinetics, Elsevier, Amsterdam, Holland, 2016.
[59] A. Jouyban, W.E. Acree Jr, Mathematical derivation of the jouyban-acree model to represent solute solubility data in mixed solvents at various temperatures, J. Mol. Liq. 256 (2018) 541–547.